EUROFUSION WPJET1-PR(16) 15831

F Clairet et al.

Plasma turbulence measured with fast frequency swept reflectometry in JET H mode plasmas

Preprint of Paper to be submitted for publication in
Nuclear Fusion

This work has been carried out within the framework of the EUROfusion Consortium and has received funding from the Euratom research and training programme 2014-2018 under grant agreement No 633053. The views and opinions expressed herein do not necessarily reflect those of the European Commission.

Plasma turbulence measured with fast frequency swept reflectometry in JET H mode plasmas

F Clairet[1], A Sirinelli[2,3], L Meneses[4] and JET contributors[*]

EUROfusion Consortium, JET, Culham Science Centre, Abingdon, OX14 3DB, UK
[1] CEA, IRFM, F-13108 St. Paul-lez-Durance cedex, France
[2] ITER Organization, Route de Vinon-sur-Verdon, CS 90 046, 13067 St. Paul Lez Durance Cedex, France.
[3] Fircroft Engineering, Lingley House, 120 Birchwood Point, Birchwood Boulevard, Warrington, WA3 7QH, UK
[4] IPFN, IST, Universidade de Lisboa, 1049-001 Lisboa, Portugal

[*] see the appendix of Romanelli F. et al (2014 Proc. of the 25th IAEA Fusion Energy Conf. (Saint Petersburg, Russia, 13–18 October 2014)).

Abstract

In this work we present recent achievements to provide precise measurements of turbulence on JET H mode plasmas using frequency sweeping reflectometry diagnostic. The plasma density fluctuations retrieved from swept reflected signals, first initiated with the Tore Supra reflectometry [1-3], provides a localized and continuous radial determination of the density fluctuation level and its spectral structure. Using the complete set of the JET X-mode fast sweeping heterodyne reflectometers we have determined the temporal dynamic of the density fluctuation profile from the edge to the center during an H mode discharge. At the L-H transition, the turbulence reduction has been evaluated to occur near the edge ($\rho \sim 0.95$) and then propagates toward the center with a steepening of the wavenumber spectra. During an edge localized mode (ELM) event, a substantial density fluctuations increase has been observed with a localized turbulent wave front propagating toward the center accompanying a particle transport. We also show that type-III ELMs maintain a steady and high level of plasma turbulence compare to type-I.

1. Introduction

Plasma turbulence is strongly suspected to play a major role in the anomalous particle and heat transport, thus affecting the quality of the confinement. Also, more precise measurements of the turbulence characteristics will lead to a better understanding of this transport from the parameters governing the efficiency of a fusion device. The discovery of the transition from low confinement (L mode) to high confinement (H mode) as led to an important improvement on plasma performance. This performance is enhanced through the formation of a narrow region that supports steep gradients of density and temperature, at the edge of the plasma. A steep pressure pedestal then grows until it either saturates or is rapidly destroyed by an edge-localized mode (ELM). There has been substantial evidence that the suppression of turbulence is the consequence of the formation of a sheared flow layer [4]. First observations of a turbulence modification during the L-H transition were achieved with reflectometry [5, 6], which is a highly sensitive diagnostic to record small plasma changes. It is a non-perturbative diagnostic and as long been suitable to probe the plasma. It is not sensitive to radiations, has a small impact onto the machine and can easily be placed away. Historically, fixed frequency systems where developed to measure the plasma density fluctuations from the scattering of microwaves [7]. Thanks to frequency locking systems, which provide a high frequency stability and a narrow video frequency bandwidth these systems provide a high signal to noise ratio (S/N) [8]. They are thus particularly well suited to measure the small fluctuations of the reflected signal created by the plasma density fluctuations. However, probing frequencies can only be launched in a stepwise way preventing a tight radial mapping of the plasma. Swept reflectometers formerly dedicated to radial

density profile measurements, while having an intrinsic lower S/N, can however provide a continuous radial probing of the plasma with nowadays a high temporal resolution as fast as few microseconds [9]. The present work is an application of the technique developed in reference [2] to the JET fast frequency swept reflectometry system (KG10) installed in 2009 [10] to determine the plasma density fluctuation profiles and its evolution during the discharge.
After a short description in section 2 of the JET sweeping reflectometer systems we recall in section 3 the method used to calculate density fluctuation profiles from a frequency swept signal with its application to the JET reflected signals. We detail how it can provide a complete description of the density fluctuations from the edge to the core of the plasma. Section 4 is dedicated to the experimental results, its application to an H mode discharge with the behavior of the turbulence during the L-H transition and also during ELM crashes. Finally, the weaknesses and the strengths of this technique are discussed in section 5.

2. Description of the JET fast-swept reflectometry systems

The description of the JET reflectometers has been extensively done in [10]. The emitting and receiving antennas are located in the equatorial plane at the low field side into the vacuum vessel. For the present work we have processed only the X-mode (the electric field of the probing wave is perpendicular to the plasma magnetic field) reflectometers for coherence, simplicity and because they conveniently access a wide region of plasma from the very edge to the center. Q (upgraded in U band), V, W and D bands, which provide a frequency coverage from 40 to 150 GHz, can thus be analyzed together as a whole. Frequency sweeping are performed in 10µs with at best a minimum dead time of 5µs in between two consecutive sweeps. In-phase and quadrature-phase (I.Q.) heterodyne signals, providing separate measurements of the amplitude and the phase, are recorded at a sampling rate of 200 MHz. About 100 000 sweeps can be acquired at a versatile sampling rate, which can be varied when necessary to improve the temporal resolution at given times during the discharge.

3. Calculation of the density fluctuations from FMCW reflectometer

3.1 From phase fluctuations to density fluctuations

The reflectometer signal coming out the detector can be written as:

$$S(r,F) = A(r,F).\, e^{-i\varphi(r,F)} \tag{1}$$

Where A(r,F) is the amplitude and $\varphi(r,F)$ the phase delay recorded during the wave of frequency F propagating radially into the plasma. The radial dependence of the phase is then:

$$\varphi(r,F) = \frac{2\pi F}{c}\int_{r_0}^{r_c} N_X(r)dr \tag{2}$$

With r_c the cut-off layer, r_0 the plasma edge and N_x the X-mode refractive index. The probing wave is sensitive to the plasma refractive index which, in the case of the X-mode polarization, is a function of the density and the magnetic field. Considering the magnetic fluctuations as negligible, the signal fluctuations originate from the density fluctuations or more exactly the fluctuations of the refractive index induces phase fluctuations of the reflected signal.

$$N_X(\langle n_e\rangle + \delta n_e) \sim N_X + \delta N_X \;\rightarrow \langle\varphi\rangle + \delta\varphi \tag{3}$$

The mean phase is used to reconstruct the density profiles while the phase fluctuations arise because of the Bragg scattering process experienced by the probing electromagnetic wave along its propagation path when the following condition satisfies:

$$\overrightarrow{k_f} = -2\,\overrightarrow{k_i} \tag{4}$$

Where k_i is the incident probing wavenumber and k_f is the plasma fluctuation wavenumber.

The radial wavenumber power spectral density of the phase fluctuations of the reflected signal is then the square of the FFT of the radial dependence of the phase:

$$S_{\delta\varphi}(k_r) = \left| \int_{r1}^{r2} \delta\varphi(r).\, e^{ik_r.r}\, dr \right|^2 \tag{5}$$

This spectrum can be determined over a restricted radial extent and by sliding this radial interval we provide a radial description of the turbulence.

Contrary to the O-mode polarization, there is no analytical relationship between the phase and the density fluctuations. This relationship is then calculated using a full-wave code. According the radial propagation of the wave, it is assumed that the code can be calculated in only one dimensional (1D) to give a fair, while not complete, representation of the fluctuations. Another argument in favor of the 1D approximation, and not least, is that 2D or 3D codes are too much time consuming to be routinely processed for frequency swept reflectometers, i.e., for each sweeps and many different radial positions. It leads to solve the Helmholtz equation:

$$\left[\frac{d^2}{dr^2} - k_0^2 N_X^2(r) \right] E(r) = 0 \tag{6}$$

where k_0 is the vacuum wavenumber. The inputs of the code for the refractive index calculation are: the experimental electron density, the calculated magnetic field and the simulated density fluctuations profiles. The output is the phase fluctuating signal. It thus provides the transfer function T which relates the phase to the density fluctuation power spectra as function of the radial wavenumber.

$$S_{\delta n_e}(k_r) = T(k_r)\,.\, S_{\delta\varphi}(k_r) \tag{7}$$

The density profiles are given by the reflectometers themselves and then provide coherence for the radial locations of the fluctuations measurements. Radial uncertainties of the density profiles of typically R +/- 1cm (~rho +/- 0.01) are due the fluctuations of the reflected signal (fluctuation of the phase) mainly induced by the plasma edge turbulence. Because of the X-mode polarization of the probing wave, another source of error can come from the magnetic field determined from equilibrium calculation. A magnetic field correction is done by adjusting the reflectometry profiles to the integrated interferometry measurements [11].

We determine the density fluctuation level for a specific range of k_r values by integrating the power spectrum over this range:

$$\langle \delta n_e \rangle_{k1,k2} = \left[\frac{1}{k_2 - k_1} \int_{k1}^{k2} S_{\delta n_e}(k_r)\; dk_r \right]^{1/2} \tag{8}$$

The simulated density fluctuations profile is defined as a sum of coherent modes with a wavenumber shape and amplitude varying with radius. It is likely a problem of one equation with two unknowns. These two parameters are adjusted in order to be as close as possible to the expected experimental result: The radial dependence of the amplitude fluctuations goes roughly from tens of percent at the edge with a rapid decrease to tenths of percent at the center, and the wavenumber spectral dependence which is flat between 0 and $5cm^{-1}$ and decreasing beyond with k^{-3} variation. Fortunately, it has been

shown [2] that the calculated density fluctuation level from the spectrum integration is not very sensitive to the spectral shape. Moreover, the main influence of the plasma density fluctuations upon the phase signal occurs close the cut-off layer i.e. at low k value below 10cm^{-1}. Above 10 cm^{-1} the fluctuation level rapidly decreases by two orders of magnitude [12] and its influence on the reflected signal becomes less accurate, particularly in the plasma core when the fluctuations level goes below 1%.

3.2. Data analysis and phase fluctuation extraction

One of the key aspects is the correct extraction of the phase fluctuations from the reflected signal. It results of an adapted filtering of the beat frequency signal ($F_b = \frac{1}{2\pi}\frac{\partial\varphi}{\partial t}$). Figure 1(a) illustrates the signal processing to retrieve the signal phase: A sliding filter with a bandwidth of 20 MHz (1/10 of the total bandwidth) is then applied around the beat frequency signal. The filtering is applied to the group delay signal of the combined data of different reflectometers ($\tau = F_b / \frac{\partial F}{\partial t}$). This bandwidth has to be sufficiently narrow to reduce of the phase noise and to remove the multiple reflections which create artificial phase jumps, not too narrow in order to preserve the fluctuating signal integrity. The relevant frequency bandwidth is determined from first and last cut-off frequencies detected on the amplitude signal of figure 1(b) with suitable thresholds.

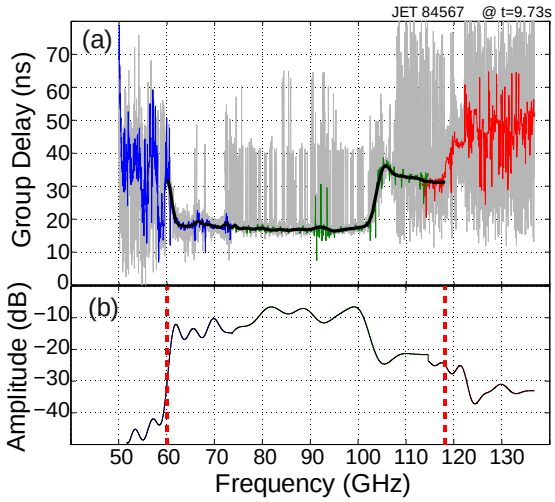

Figure 1. (a) Phase fluctuations observed from the group delay (normalized to the back wall phase reference echo) using three different reflectometers (V, W and D band). The original phase fluctuations (non-filtered signal) are in gray; the phase fluctuations of the suited filtered signal are colored by frequency bands. The black thick line corresponds to a smoothing of the group delay and represents the averaged phase which will be used to reconstruct the density profile. (b) The relevant plasma cut-off frequency interval (in between vertical dashed lines) is determined from the reflected amplitude signal for amplitude levels above -25dB in the present case.

3.3. 1D code description (inputs…)

In order to account for realistic experimental conditions for the transfer function, the measured density and the calculated (EFIT) magnetic profiles are used. A turbulence sample q is defined as:

$$\delta n_e^q(r) = f(r) \sum_{n=1}^{N} g(nk_{min}, r).\sin(nk_{min}.r + \Phi_q) \qquad (9)$$

The radial dependences of the f and g functions are defined as to fit as close as possible the final results : Figure 2 represents f(r), the amplitude envelope of the radial distribution of the fluctuations, which is forced to zero at the very edge and varies from 10% close the separatrix to 0.1% in the center in order to fit the amplitude data. g(k,r) is the wavenumber spectrum with a radial dependence varying from $k^{-0.1}$ at the edge to k^{-4} at the center. Φ_q are the random phases for q samples. These values have been selected out after several attempts and runs to provide satisfactory convergence between the input and output of the radial dependence of the turbulence amplitude and spectrum.

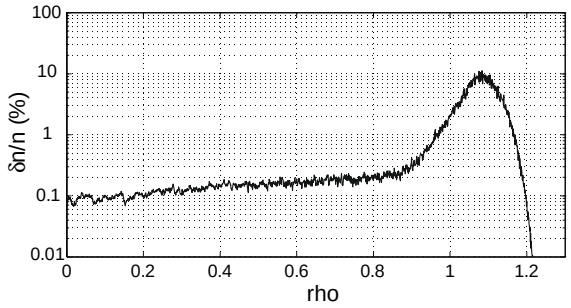

Figure 2. Averaged amplitude over 50 samples of density fluctuation profiles introduced into the Helmholtz 1D code for the calculation of the transfer function.

In our calculation, the transfer function is statistically evaluated using N=50 samples are used to determine the relation between the density fluctuations and the phase fluctuations of the reflected signal. The number of samples used is a compromise between the acceptable signal to noise ratio and the computational time.

$$T^{simu} = \frac{\langle S^{simu}_{\delta n_e} \rangle_{50}}{\langle S^{simu}_{\delta \varphi} \rangle_{50}} \tag{10}$$

The determination of the density fluctuation level is also performed statistically to improve the S/N ratio, and a compromise has to be found between the time resolution (number of N recorded signals) and the S/N ratio.

$$S^{exp}_{\delta n_e}(k_r) = T^{simu}(k_r) \; . \; \langle S^{exp}_{\delta \varphi}(k_r) \rangle_N \tag{11}$$

3.4. Calculation (radial resolution/integration, kr spectrum integration…)

The wavenumber of a probing wave varies from k_0 ($2\pi F/c$) at the edge to 0 at the cut-off layer and, according the Bragg law, it backscatters on the plasma density fluctuations at twice these values. The radial dependence of the probed wavenumber fluctuations is illustrated on figure 3 for three different probing frequencies. We see that in order to provide a good radial resolution close the cut-off layer, the integration of the density fluctuations spectra must be restricted to low k values. For the determination of the density fluctuation level, we integrate the power spectra up to 10 cm^{-1}, which thus provide a localized measurement close the cut-off.

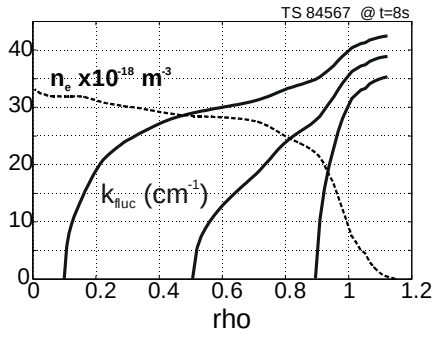

Figure 3. Probed fluctuation radial wavenumbers according three different probing frequencies (84.6, 93.1 and 101.6 GHz) with respective cut-off positions at rho = 0.9, 0.5 and 0.1. The density profile is represented in dotted lines.

On the other hand, the minimum measurable wavenumber of the fluctuations is given by the radial window width (k_{min} = 2 x 2π/Δr) used for the phase spectrum calculation, and a compromise as to be found between the radial resolution and the lowest wavenumber extent of the density fluctuations power spectra as shown figure 4(a). Thus, different fluctuation levels can thus be found according the integrating wavenumber range of the spectra but it generally leads to a shift of the whole fluctuation profile as shown on figure 4(b).

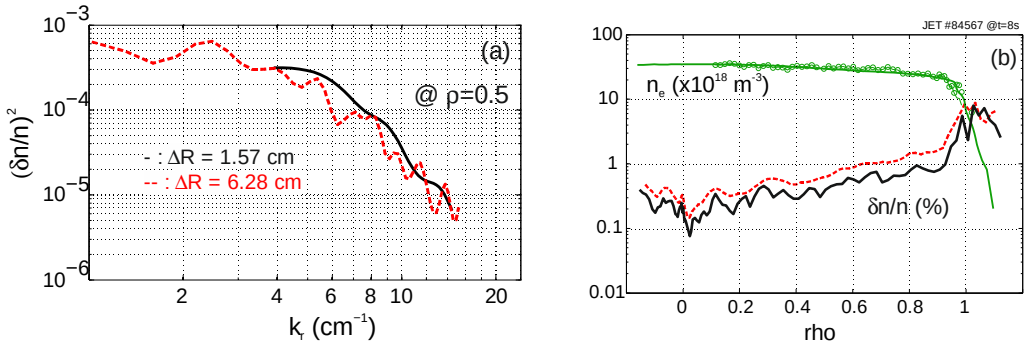

Figure 4. These results have been obtained in the ohmic phase using 100 measurements: (a) power spectra of the density fluctuations calculated at ρ=0.5 using different radial window widths of 1.57cm (full line) and 6.28cm (dashed line). (b) Fluctuation density profiles calculated with the two different window widths. Are represented as well the density profiles measured with reflectometry (full line) and Thomson scattering (circles).

4. Experimental results

The choice of the JET discharge 84567 has been done as it covers a large range of physical processes (figure 5(a)). It contains an L-H transition which occurs around 8.65s after the NBI additional power is turned on, followed by a series of type-I ELMs up to 9.5s, then type-III ELMs up to the end of the NBI power with a short ELM free period in between. Due to the limited memory capacity of the acquisition, the maximum recordable signals/profiles is 100 000 per discharge, thus in order to optimize it, the sampling rate of the reflectometers (figure 5(b)) has been decreased to 1 sweep every 60μs during the H mode phase down to the highest rate (15μs) between 9 and 9.5s during the type-I ELMs.

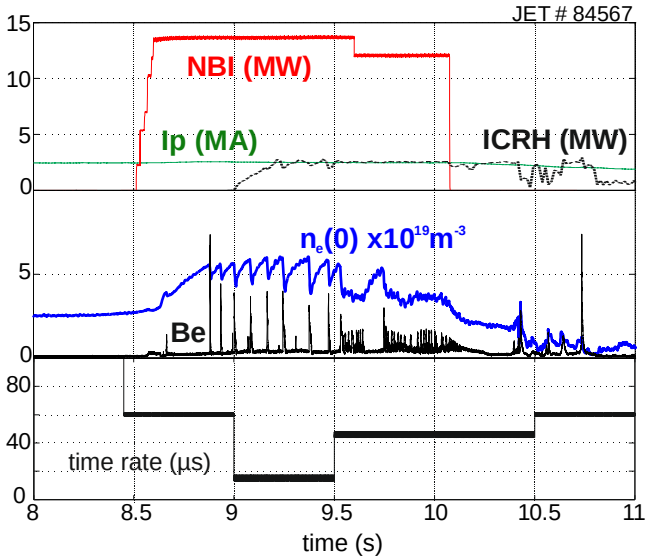

Figure 5. Plasma timeline of the JET discharge 84567. L-H transition occurs at about 8.6s after neutral beam power is turned on; The ELM activity (in black) is recorded through the emission of the Be II signal at the outer divertor. It starts with a type-I ELM activity and turns to type-III at about 9.55s followed by a short 100 ms ELM free period and again type-III activity until the end of NBI power. Sampling rate (time between sweeps) of the fast swept reflectometers is varied during the discharge (before 8.5s the sampling rate is 1ms).

4.1. L-H transition

The swept reflectometers first provide the radial density profile which will give the correspondence between the radii and the cut-off frequencies for the localization of the turbulence measurements. The consequence of the transition to the H mode at 8.65s is an abrupt increase of the plasma density as seen on the 3D plot (figure 6) with a strong steepening of the edge profile also called the pedestal region and a flattening in the core.

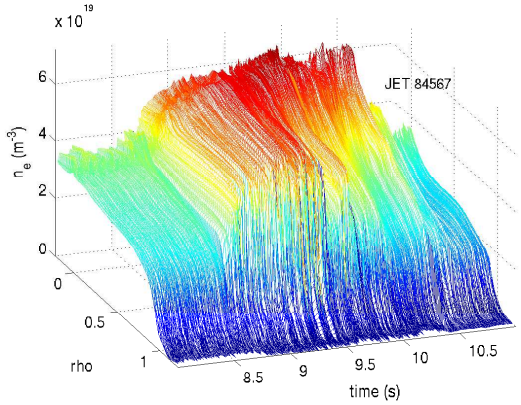

Figure 6. Density profile evolution of plasma discharge 84567.

By applying the turbulence analysis process onto the reflected signal fluctuations, we show on figures 7 an overview of the radial and temporal behavior of the turbulence. In order to cover a rather broad time range of the discharge in a reasonable amount of time (here about 10 hours of calculation), the calculation has been achieved with one profile every 5ms. In order to improve the signal to noise

ratio, several consecutive sweeps have been used to recover one profile and, remarkably, this can be achieved with a rather low number of frequency swept signals (5 signals in this case).

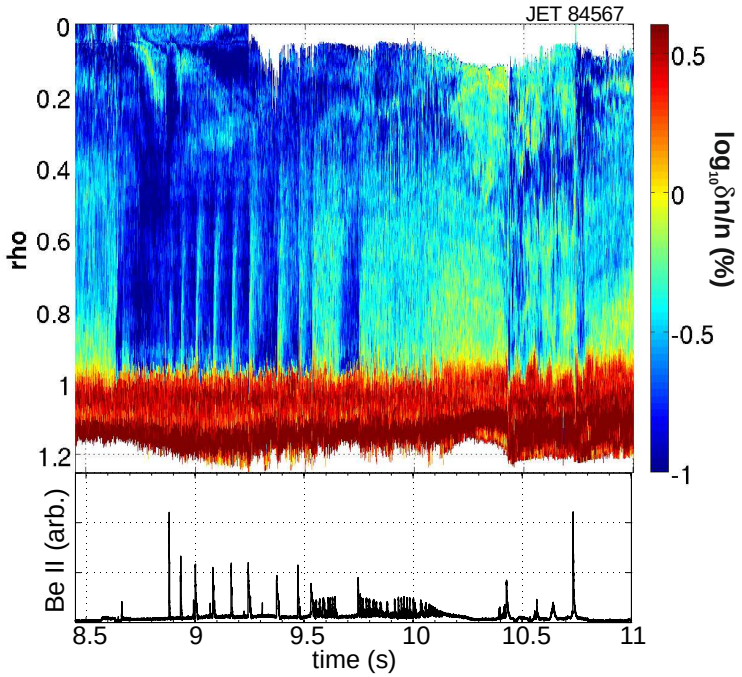

Figure 7. Temporal evolution of the radial density fluctuation profile at a time resolution of 1ms (using 5 signal sweeps to calculate one profile). The radial window of integration is 1.57cm. The L-H transition occurs at t ≈ 8.65s. The color bar indicates the percentage of the fluctuation level δn/n in logarithmic scale. The bottom black line represents the emission of the Be II signal at the outer divertor, standing for the ELM activity.

We first see that the L-H transition at 8.63s is characterized by a strong reduction of the fluctuation level from the plasma edge to the core. At 8.66s a first ELM occurs and the turbulence temporarily increases along with a small density drop then the H mode recovers. From 8.88s a type-I ELMs regime happens, each ELM induces intermittent turbulence increases with a density drops. In between theses ELMs the turbulence drop again and the density rise up which confirms what has been previously observed [13]. Then at 9.5s a type-III ELMs regime leads this time to an increase of the plasma turbulence up to almost mid-radius that keeps at high level along with a steady density drop. A short ELM free period of about 100ms from 9.65s to 9.75s exhibits a turbulence drop and a density increase until the type-III ELM regime occurs again until the end of neutral additional power. Beyond 10s the plasma current decrease and the plasma behavior becomes somehow chaotic and is out the scope of this study. As we get close to the separatrix and in the scrape-off layer (SOL) the turbulent level is always high (δn/n > 10%) so that the signal phase response become strongly non-linear and no valuable information has been extracted in this region so far with this method.

In the figure 8(a) we present the L-H transition with a higher time resolution with one profile every 300µs to provide a closer look at the temporal dynamic. The turbulence profiles were calculated using 5 consecutive sweeps as the sampling rate is 60µs between 8.5 and 9s. To figure where the turbulence drop occurs, the figures 8 (b) and 8(c) compare the density and fluctuation profile before and after the L-H transition. The drop of the turbulence clearly profile occurs into the pedestal region; however, a precise radial localization within this pedestal is hard to reach. As a matter of fact, in order to perform the fluctuation calculation, a radial window of integration of ΔR=1.57cm was used which correspond to approximately Δρ~ 0.016.

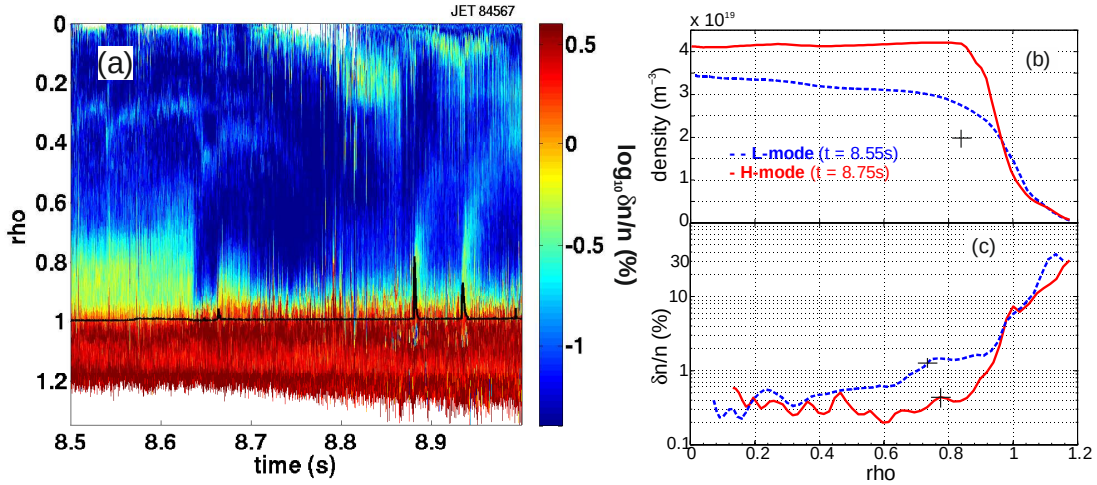

Figure 8. (a) Temporal evolutions of the radial density fluctuation with one profile every 300µs (using 5 signal sweeps per profiles) with the ELM activity superimposed in black. The radial window of integration is 1.57cm and the color bar indicates the percentage of the fluctuation level dn/n in logarithmic scale. (b) and (c) is a comparison of the density and fluctuation profiles before and during the H transition.

On figure 9(a) the turbulence starts to drop from the plasma edge between rho=0.9 – 0.95 and then propagates to the core up to mid-radius. Further in the plasma center, as the turbulence level is already low (δn/n~0.1%), no substantial turbulence modification is observed. The density modification shown on figure 9(b) is concomitant to the turbulence drop and the radial position between density rise and drop is measured at rho=0.94 +/- 0.01.

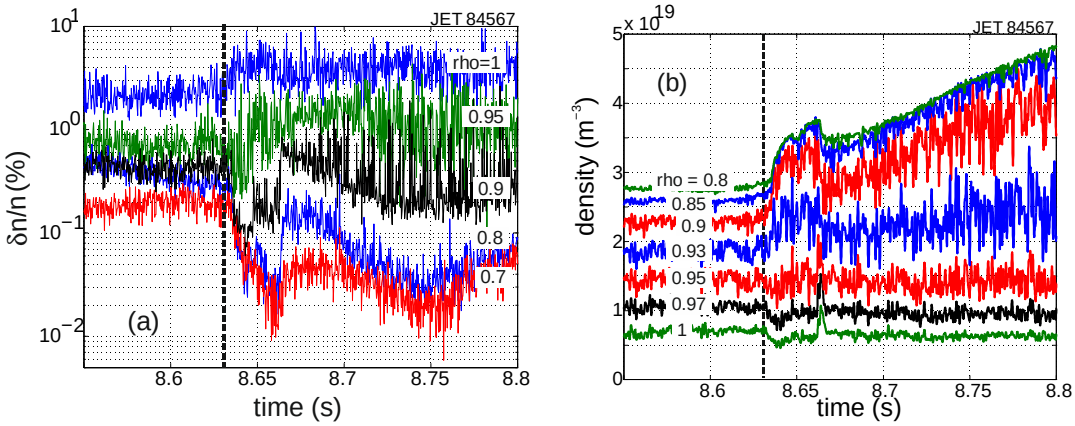

Figure 9. (a) Time evolution of the density fluctuation level at the L-H transition at different radii. Turbulence reduction first occurs around 0.95 to 0.9 and propagates toward the plasma center. (b) Time evolution of the edge density at the L-H transition for different normalized radii. Density increase occurs around rho=0.94.

4.2. Wavenumber spectra

The determination of the wavenumber spectra from a reflectometry signal is not straightforward in X-mode polarization since no analytical relationship exists between the signal phase and the density fluctuations. Moreover, the shape of the spectra depends on the level of the density fluctuation. As a matter of fact, strong fluctuation levels generate multiple wave scatterings that create a non-linear response of the probing wave. There is then an energy transfer from low k to high k into the spectrum

[14] which, however, influences the shape rather than the integrated amplitude [2]. It has been shown that these non-linear effects arise as the density fluctuation level exceeds 1%.
As quoted in reference 2, and confirmed in this analysis, a proper spectrum characterization requires of the order of 100 to 200 frequency swept signals, which is 20 to 40 times what is needed for the determination of a fluctuation profile. Moreover, a broad integrated radial window provides a larger number of measuring points and allows a better spectrum characterization but at the expense of the radial resolution.
Figure 10(a) shows a comparison between L and H mode power spectra in the plasma core, at ρ=0.6, where the density fluctuation is well below 1% (figure 8(c)) while figure 10(b) shows the calculated radial evolution of the spectral index calculated from the spectra slope between 2 and 10 cm^{-1}. While the slopes of the spectra do not exhibit firm k power dependence, along with a decrease of the turbulence level in H mode, a substantial steepening of the spectra is observed from the edge up to the center. The modification of the spectral slope can be related to non-linear effects of the density fluctuations onto the phase fluctuations of the reflected signal. This is probably true at the edge where the plasma turbulence is high, however, the linear relationship between phase and density fluctuations should be more solid toward the plasma core where the fluctuation level is low (δn/n< 1%). However, in the plasma center, where no change of the turbulence amplitude is observed, there is still a modification of the spectral shape. Comparisons with perpendicular wavenumber spectra [12, 15] have been done, they are mainly measured from Doppler backscattering systems and generally exhibit steeper slopes.

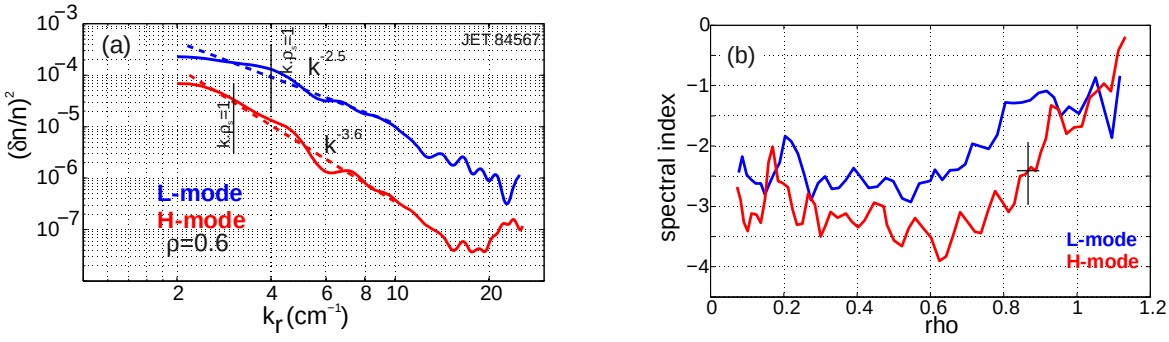

Figure 10. (a) Wavenumber density fluctuation spectra comparison between ohmic and H mode at ρ=0.6 (calculated with a radial window dR=3.15cm and averaged from 200 sweeps). (b) Radial dependence of spectral index of L and H modes (the slopes are calculated between 2 and 10 cm^{-1}).

4.3. ELM event

In H mode operation, short, repetitive magnetic instabilities, known as ELMs, are observed to transport bursts of heat and particles across the pedestal. A type-I ELM is a relatively isolated event and its radial and temporal evolution can thus be conveniently described. Figure 11(a) shows the density profile as the ELM occurs around 9.37s. At the crash, a substantial amount of plasma density is expelled and then edge profile recovers slowly. On figure 11(b) a turbulent burst is visible and propagates toward the core at roughly 50m/s and slowing down up to mid-radius. In the meantime this burst causes a turbulence increase at least up to mid-radius. Along with figure 11(c), this turbulent wave front goes with the density collapse and the density profile recovers as the turbulent front dissipates.

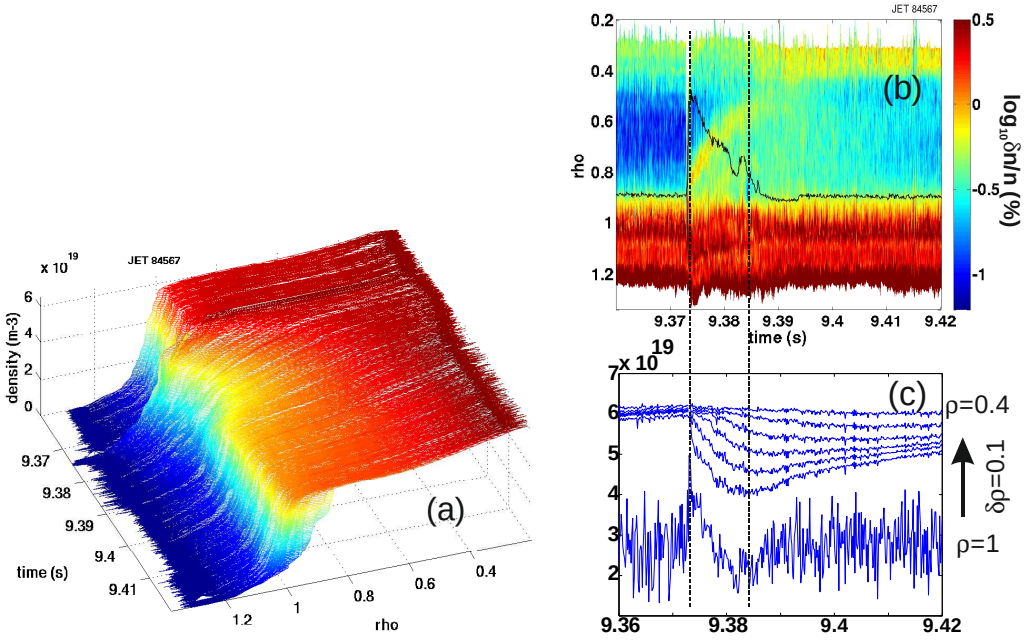

Figure 11. Measurements during a type-I ELM : (a) Density profile evolution. (b) Density fluctuations (each profile is calculated from 10 signals and window width dR=3.14cm) radial propagation after the ELM crash compared to (c) the density evolution from ρ=1 to 0.4 by steps of δρ=0.1.

It appears that the turbulence behavior during the type-I ELM can be extrapolated to type-III EMLs one observed in figure 7. In fact during type-III the turbulence is kept at a high level thanks to the high repetitive rate of the crashes and we observed that the density steadily decreases and does not recover. This might be the reason of the lowest plasma confinement efficiency observed with type-III ELMs compare to type-I [16, 17].

5. Summary and discussion

In this work, we have shown that the fast swept reflectometry is a powerful tool to measure the plasma density fluctuations. The data processing of swept reflected signals lets to provide a temporal and radial description of the fluctuation profile from the edge to the core of the plasma. Relevant information on the variation of the density fluctuation level can be determined using few sweeps of about 5 to 10, while a proper resolution of the wavenumber spectral shape requires about 100 to 200 sweeps. We consider that a radial integration of 3.14cm is a good compromise to provide a fair description of the spectra with sufficient number of phase fluctuating points, while the fluctuation level is well determined with a radial integration down to 1.57cm. While the relationship between the plasma and the signal fluctuation is not always straightforward, particularly during high turbulence level conditions, the variations and evolutions of the turbulence with respect to any change in the confinement regimes and configuration make sense. Thus, turbulent changes during an L-H transition as well as during ELM crashes have been clarified. We have shown that at the L-H transition the fluctuation reduction starts from the edge around ρ≈0.95 and propagates towards the core of the plasma. The turbulence reduction occurs mainly on the outer half of the plasma and in the plasma center, where the fluctuation level is already low (δn/n~0.1%), no significant modifications were observed.

Regarding the ELM, when the crash occurs, a turbulent front arises at the plasma edge and propagates towards the core. This front induces a temporary increase of the edge turbulence up to at least mid-radius which then fades away. This turbulence rising is accompanied by an enhanced transport as the density fall. Due to its high repetition rate, type-III ELMs keeps a steady and relatively high edge turbulence level while with type-I ELMs the turbulence level has the time to return to a low level in

between each crashes. This can provide an explanation for the better confinement efficiency obtained with low frequency type-I compared to type-III. An ELM free regime also exhibits a turbulence reduction which seems to be nothing else that what is observed in between type-I ELMs but with a longer time which also provides a better confinement.
The determination of the wavenumber spectral shape remains delicate since it may be substantially flattened due to nonlinear interactions between the probing electromagnetic wave and the plasma fluctuations at high level. At the last closed flux surface and beyond in the scrape-off layer, where the turbulence level is high and intermittent, no clear information can be sorted out. In this far edge region these characteristics are not taken into account in our turbulent model and an effort should be done for a better account of the non-linear wave response. Despite these considerations, a clear steepening of the spectra is observed when going from L to H mode in the plasma core even where no turbulence reduction is observed.
In future plan and using an extended data set, this method will be suited to provide a parametric scaling of the turbulence.

Acknowledgement

This work has been carried out within the framework of the EUROfusion Consortium and has received funding from the Euratom research and training programme 2014-2018 under grant agreement No 633053. The views and opinions expressed herein do not necessarily reflect those of the European Commission. The views and opinions expressed herein do not also necessarily reflect those of the ITER Organization

References

[1] Heuraux S, Hacquin S, da Silva F, Clairet F, Sabot R, Leclert G 2003 *Rev. Sci. Instrum.* **74** 1501
[2] Vermare L, Heuraux S, Clairet F, Leclert G and da Silva F. 2006 *Nucl. Fusion* **46** S743
[3] Gerbaud T, Clairet F, Sabot R, Sirinelli A, Heuraux S, Leclert G and Vermare L, 2006 *Rev. Sci. Instrum.* **77** 10E928
[4] Wagner F 2007 *Plasma Phys. Control. Fusion* **49** B1
[5] Doyle E J, Groebner R J, Burrell K H, Gohil P, Lehecka T, Luhmann N C, Matsumoto H, Osborne T H, Peebles W A and Philipona R 1991 *Physics of Fluids* **B3** 2300
[6] Manso M 1993 *Plasma Phys. and Control. Fusion* **35** B141
[7] Mazzucato E 1976 *Phys. Rev. Letter* **36** 792
[8] Laviron C, Donné A J H, Manso ME and Sanchez J 1996 *Plasma Phys. Control. Fusion* **38** 905
[9] Clairet F, Heuraux S, Bottereau C, Molina D, Ducobu L, Leroux F, and Barbuti A 2010 *Rev. Sci. Instrum.* **81** 10D903
[10] Sirinelli A. et al. 2010 *Rev. Sci. Instrum.* **81** 10D939
[11] Belonohy E *et al.* 2014 *Report EFDA-JET-CP(14)05/18*
http://www.euro-fusionscipub.org/wp-content/uploads/2014/11/EFDC140518.pdf
[12] Hennequin P, Honoré C, Truc A, Quéméneur A, Fenzi-Bonizec C, Bourdelle C, Garbet X, Hoang GT and the Tore Supra team 2006 *Nucl. Fusion* **46** S771
[13] Soldatov S, Krämer-Flecken A, Kantor M, Unterberg B, Sun Y, Van Oost G, Reiter D and the TEXTOR team 2010 *Plasma Phys. and Control. Fusion* **52** 85001
[14] Bruskin L G, Oyama N, Mase A, Shinohara K and Miura Y 2004 *Plasma Phys. Control. Fusion* **46** 1313
[15] Casati A *et al.* 2009 *Phys. Rev. Lett.* **102** 165005
[16] Sartori R, Saibene G, Horton L D, Becoulet M, Budny R, Borba D, Chankin A, Conway G D, Cordey G, McDonald D 2004 *Plasma Phys. Control. Fusion* **46** 723
[17] Osborne T H, Groebner R J, Lao L L, Leonard A W, Maingi R, Miller R L, Porter G D, Thomas D M, and Waltz R E 1997 *Proceedings of the 24th European Physical Society Conference on Controlled Fusion and Plasma Physics, Berchtesgaden* **21A** 1101